Published in final edited form as:
Anal Chem. 2006 March 1; 78(5): 1528–1534. doi:10.1021/ac052067g.

Quantitative Detection of Individual Cleaved DNA Molecules on Surfaces Using Gold Nanoparticles and SEM Imaging

Bei Nie, **Michael R. Shortreed**, and **Lloyd M. Smith***
Department of Chemistry, University of Wisconsin-Madison, 1101 University Avenue, Madison, Wisconsin 53706, USA

Abstract

Single nucleotide polymorphisms (SNPs) are the most frequent type of human genetic variation. Recent work has shown that it is possible to directly analyze SNPs in unamplified human genomic DNA samples using the surface invasive cleavage reaction followed by rolling circle amplification (RCA) labeling of the cleavage products. The individual RCA amplicon molecules were counted on the surface using fluorescence microscopy. Two principal limitations of such single-molecule counting are the variability in the amplicon size, which results in a large variation in fluorescence signal intensity from the dye-labeled DNA molecules, and a high level of background fluorescence. It is shown here that an excellent alternative to RCA labeling is tagging with gold nanoparticles followed by imaging with a scanning electron microscope (SEM). Gold nanoparticles have a uniform diameter (15±0.5 nm) and provide excellent contrast against the background of the silicon substrate employed. Individual gold nanoparticles are readily counted using publicly available software. The results demonstrate that the labeling efficiency is improved by as much as ~15 fold and the signal-to-noise ratio is improved by ~4 fold. Detection of individual cleaved DNA molecules following surface invasive cleavage was linear and quantitative over three orders of magnitude in amount of target DNA (10^{-18}–10^{-15} moles).

Single nucleotide polymorphisms (SNPs) are important and abundant genetic variations in the human genome sequence.[1–4] Identification of these genetic differences is useful for understanding how allelic variation underlies susceptibility to common diseases [5,6]. The invasive cleavage reaction is a powerful tool for the analysis of genetic variation.[7,8] In invasive cleavage reactions, a three dimensional structure is formed by hybridization of two partially overlapping synthetic DNA oligonucleotides to a target DNA strand.[9] A flap endonuclease (FEN) specifically recognizes this structure and cleaves a flap from the 5′ end of the downstream synthetic probe (Figure 1). The cleavage rate is approximately 300 times greater for probe oligonucleotides that are complementary at the point of cleavage compared to those that are not. This attribute of the FEN enzyme confers single nucleotide specificity to the cleavage reaction. [10] Each target molecule can participate in multiple cleavage events, which provides a mechanism for signal amplification without a requirement for PCR amplification of the target DNA.[11]

This approach may be parallelized by fabrication of a DNA array in which the two different synthetic oligonucleotides that are required for the invasive cleavage reaction are immobilized within each array element. [12] Addition of target DNA permits formation of the specific invasive cleavage complex at each array site followed by specific cleavage. A significant advantage of this approach to large-scale SNP analysis is that all of the oligonucleotides needed

* To whom correspondence should be addressed. Phone: (608) 262-9207. Fax: (608) 265-6780. E-mail: smith@chem.wisc.edu. Internet: http://www.chem.wisc.edu/~smith.

may be synthesized in parallel on the support using array fabrication technologies. The simple addition of target DNA, enzyme, and buffer to the array, followed by incubation, washing, and detection steps, reveals the genotype of the target DNA for every SNP site included in the array.

A key issue in high throughput SNP analysis is detection sensitivity. This is important because the amount of human genomic DNA sample available for genetic studies is often limited in quantity. Rolling circle amplification coupled with universal ligation of RCA primers has been used to enhance the signal from the surface invasive cleavage reaction. Rolling circle amplification produces long single-stranded DNA products [13] that can be stained with fluorescent dye to yield a large fluorescence signal. The RCA products are long enough that individual cleavage events can be detected using single molecule microscopy.[14] However, there is a significant variability in the length of individual amplicons and it can be difficult to conclusively identify individual cleavage events; for example, when two amplicons are produced within a distance from one another that is not optically resolvable. In addition, the fluorescent dye used to detect the RCA products can produce significant background fluorescence, compromising the detection of shorter RCA amplicons.

In the present work an alternative detection strategy is employed, which makes use of gold nanoparticle labels and permits the identification of individual surface cleavage events with extremely uniform signal and low background interference.[15,16] Products of the cleavage reaction (5′ phosphate groups) are ligated to biotinylated oligonucleotides using universal degenerate templates.[12] Streptavidin-conjugated gold nanoparticles are then coupled to the surface-bound biotinylated probes followed by visualization with a scanning electron microscope (SEM). The nanoparticles are highly monodisperse with standard deviations in their diameter of <10%. This excellent monodispersity produces uniform electron backscattering intensity from each particle.[17,18] The efficiency of the nanoparticle labeling procedure is improved by as much as 15 times over the RCA labeling procedure. Gold nanoparticles imaged by SEM are readily counted with high accuracy and confidence using freely available computer software packages whereas fluorescently tagged RCA amplicons are not amenable to such automated counting. Finally, the nanoparticle labeling scheme was used for the detection of individual cleaved DNA molecules following the surface invasive cleavage assay. The detection is linear and quantitative over three orders of magnitude in concentration.

EXPERIMENTAL SECTION

Chemical Reagents and Oligonucleotide Sequences

The following sequences were designed for genotyping a single nucleotide polymorphism (W1282X) in the cystic fibrosis transmembrane conductance regulator (CFTR) gene 23. We note that W1282X is formally a mutation rather than a SNP, as SNPs are defined as polymorphisms for which the minor allele frequency is at least 1% [19]. However, as a single nucleotide variation of substantial medical consequence, it was chosen here as a model system. Invader oligonucleotide: 5′-GCT CAC CTG TGG TAT CAC TCC AAA GGC TTT CCT A-3′; wild-type probe: 5′-Dabcyl-CCA CTG TTG CAA AGT TAT T-$(T)_{15}$-SH-3′; mutant-type probe: 5′-Dabcyl-TCA CTG TTG CAA AGT TAT TG-$(T)_{15}$-SH-3′. Synthetic target DNAs were used in these experiments. Wild-type target: 5′-GGA TTC AAT AAC TTT GCA ACA GTG GAG GAA AGC CTT TGG AGT GAT ACC ACA GGT GAG CAA AAG-3′; mutant-type target: 5′-GGA TTC AAT AAC TTT GCA ACA GTG AAG GAA AGC CTT TGG AGT GAT ACC ACA GGT GAG CAA AAG-3′. Degenerate guide DNA: 5′-NNN NNN GCA TTC CG-3′ (where N = G,A,T,C); Biotin-oligo: 5′-Biotin-TTTTTTCGGAATGC-3′. All of the aforementioned sequences were synthesized by the University of Wisconsin Biotechnology center and purified as described previously [20]. The two sequences used for the determination of detection efficiency (mixed 5′-biotin and 5′-dabcyl) were: 5′-Biotin-(TEG)-TCA CTG TTG

CAA AGT TAT TG-$(T)_{15}$-SH-3′; and 5′-Dabcyl-TCA CTG TTG CAA AGT TAT TG-$(T)_{15}$-SH-3′. These two oligonucleotides were obtained in PAGE purified form from Integrated DNA Technologies (Coralville, IA). The heterobifunctional linker sulfosuccinimidyl 4-(N-maleimidomethyl) cyclohexane-1-carboxylate (SSMCC) was obtained from Pierce (Rockford, IL). T4 DNA ligase was purchased from New England Biolabs (Beverly, MA). Streptavidin-coated gold colloid (15 nm diameter) was ordered from Ted Pella (Redding, CA). SSC buffer was purchased from Ambion (Austin, TX). Silicon wafers ((111) crystal face, n-type arsenic-doped) were purchased from Virginia Semiconductor (Fredericksburg, VA) and cut to 5 mm × 7 mm dimensions.

Invasive Cleavage Reaction

The invasive cleavage reaction is a sensitive and specific assay for detecting single-nucleotide substitutions[7,10] that involves hybridization of two synthetic oligonucleotides to a single-stranded DNA target followed by cleavage of one of the synthetic sequences by a structure-specific 5′-endonuclease. The sequence that hybridizes upstream of the single-nucleotide substitution is referred to here as the invader and the sequence that hybridizes downstream of the single-nucleotide substitution is referred to here as the probe. The nucleotide at the 3′ end of the invader oligonucleotide is designed to overlap at least one base into the downstream duplex formed by the probe and the target strand. The unpaired region on the 5′ end of the probe, or “flap”, along with an immediately downstream paired nucleotide is then removed by the flap endonuclease. Absolute complementarity between the probe and the target sequence at the position of overlap is required for efficient enzymatic cleavage. The cleavage reaction yields a free 5′-phosphate moiety on the probe oligonucleotide, which may be detected in a subsequent labeling reaction as described below.

Surface Invasive Cleavage Reaction

The surface invasive cleavage assay has been performed in two different formats[21]. In one format, both probe and invader oligonucleotides are co-immobilized on the reaction substrate. In the other format only the probe is immobilized on the solid substrate and the invader oligonucleotide is added with other reaction components. The latter format was employed for this study (Figure 1). The reaction mixture consisted of 1 μL of synthetic target DNA and 10 μL of reaction buffer (10 mM MOPS, pH, 7.5 mM $MgCl_2$, 250 nM invader oligonucleotide, and 50 ng Afu FEN (Cleavase X, Third Wave Technologies, Madison, WI)). The concentration of the added target depended on the experiment. The reactions were performed in a humid chamber at 58.5 °C for 3 h. The slides were then rinsed with water and soaked in 8 M urea for 10 min at 37 °C. This was followed by another thorough rinse of the slides with water.

Preparation of Amine-terminated Silicon Substrates

The surface of silicon wafers was first cleaned in piranha solution (4:1 concentrated H_2SO_4 (Fisher, Trace Metal Grade): 30% H_2O_2) and then rinsed with 1:1:4 30% H_2O_2, concentrated HCl, and H_2O at 80°C for 20 minutes. Caution: Piranha solution is extremely dangerous when prepared and handled improperly. This was followed by a thorough rinse in deionized water. Next, the silicon chip was terminated with hydrogen by immersion in a solution of 40% NH_4F for 20 min [22]. The hydrogen terminated silicon substrates were then washed with water and dried under a nitrogen stream. A thin layer of TFAAD (trifluoroacetamide-protected 10-aminodec-1-ene) was sandwiched between the silicon substrate and a quartz cover-glass. The silicon substrate was exposed to UV light (254 nm, 0.35 mW/cm^2) through the quartz for 12 h in a chamber that was continuously purged with nitrogen gas. During this process, the olefin group of the TFAAD reacted with the surface [23]. The substrates were sonicated in $CHCl_3$ and then methanol for 5 min each. The trifluoroacetamide protecting group was removed by immersing the substrates in a solution of 0.36 M HCl in methanol for 48 h at 65 °C.

Attachment of Oligonucleotides to Amine-terminated Silicon Substrates

The amine-terminated chips were treated with 0.4 mg/mL SSMCC (sulfosuccimidyl-4-(N-maleimidomethyl) cyclohexane-1-carboxylate) in 0.1 M triethanolamine buffer (pH 7.0) for 15~20 min at room temperature. After rinsing the chips with water, 1 μL drops of 0.5 mM thiol modified DNA oligonucleotide were deposited on the substrates and permitted to react in a humid chamber overnight.

Oligonucleotide Hybridization Density

Oligonucleotide-modified substrates were incubated with 2 μM fluorescein-labeled complementary DNA in 2× SSPE/0.2 % SDS hybridization buffer for 30 min. Non-specifically attached DNA was removed from the surface by twice agitating the substrates for 5 min in a 50 mL beaker containing hybridization buffer. Complementary DNA was eluted from the substrate by placing the chip in 5 mL of 132 mM KOH/50 mM KCl for 5 min. The concentration of fluorescent oligonucleotides that were eluted from the chip was determined by comparing the fluorescence signal generated from the solution containing the eluted oligonucleotides to fluorescence signals from solutions containing known amounts of the fluorescein-modified oligonucleotide. Fluorescence from all solutions was measured using a plate reader (BIO-TEK Instruments, Inc. model Flx800, Winooski, VT). The hybridization density was calculated by determining the number of eluted oligonucleotides and dividing that number by the surface area of the substrate. Using the protocol above, the number of hybridizable DNA probes per unit area was calculated to be $(0.80\pm0.05) \times 10^{12}$ molecules/cm^2.

Detection of 5′-phosphate Groups Produced During the Surface Invasive Cleavage Reaction

The strategy for detecting the free 5′-phosphate groups that were produced in the surface invasive cleavage assay (Figure 1) consisted of two steps: degenerate ligation to a biotin-modified oligonucleotide and conjugation with streptavidin-coated gold nanoparticles. Surface bound probe oligonucleotides were synthesized with a terminal dabcyl group, which prevented non-specific ligation. A biotinylated oligonucleotide (3 μM) was ligated to the free end of the cleaved probes at 0 °C using 0.3 mM degenerate guide DNA and 1 U/μL T4 DNA ligase in buffer solution that was supplied by the manufacturer as part of the ligation kit.[24] The ligation reaction was carried out for 12 h. Substrates were rinsed with 1× SSC buffer containing 0.2% SDS and with water before being dried under a stream of nitrogen.

Streptavidin-coated gold colloids of 15 nm diameter (Ted Pella, Redding, CA) were washed twice with phosphate-buffered saline (PBS pH 7.4) that was supplemented with 0.2% Tween 20 and 1 mg/mL BSA. These colloids were then suspended in binding buffer (10 mM Tris-HCl pH 7.5, 1 mM EDTA, 0.5 M NaCl, 0.1% Tween 20) at a concentration of 10 nM. A 50 μL aliquot of the colloidal suspension was applied to each biotinylated DNA chip for 4 h in a humid reaction chamber at room temperature. Following the incubation reaction, the chips were washed three times with PBS with 0.2% Tween 20 and then rinsed with water for about 10 min. The substrates were then dried overnight.

Determination of Nanoparticle Binding Efficiency

Surfaces for the determination of nanoparticle binding efficiency were prepared as described above except that two probes were mixed together to a final concentration of 0.50 mM prior to deposition on the chip surface. The two probes were 5′-terminated either in biotin or dabcyl (see *Chemical Reagents and Oligonucleotide Sequences*). The six different biotin:dabcyl ratios employed were: 0:1; 1:1, 1:10, 1:100; 1:1000; and, 1:10000. Each of the six probe mixtures were spotted onto two separate chips.

Scanning Electron Microscopy

Backscatter from the gold-nanoparticles was visualized on the silicon substrates using a scanning electron microscope (LEO 1530, Field Emission SEM, Carl Zeiss, Inc.). Typically, four regions, 20–40 μm^2 in size, were scanned for each reaction. The number of gold nanoparticles in each image obtained was counted using the publicly available NIH Scion Image processing software (http://www.scioncorp.com). The particle surface density was calculated as the average number of particles in a frame divided by the area of each frame.

Calculations of Signal-to-Noise Ratio

Signal-to-noise ratio (S/N) calculations were performed on images of surface-bound probe oligonucleotides tagged with either fluorescently labeled RCA amplicons or gold nanoparticles. In the case of the RCA amplicons, a number of individual molecules were identified by visual inspection and their peak (brightest point) intensities S were recorded. Background intensity B was measured in the interstitial space between the amplicons. The S/N is thus $\{(S\pm \sigma_S)-(B\pm \sigma_B)\}/\sigma_B$, where σ is the standard deviation. Signal-to-noise ratio calculations for the gold nanoparticles were performed in an analogous fashion. Data from three different regions on each of four different chips (a total of 12 sections) were used for each calculated value.

RESULTS AND DISCUSSION

Comparison of the Detectability of Individual Rolling Circle Amplicons by Fluorescence Microscopy and of Gold Nanoparticles by Scanning Electron Microscopy

In previous work, rolling circle amplification (RCA) provided the necessary signal to enable genotyping of non-PCR amplified genomic DNA by surface invasive cleavage [24]. RCA amplicons were so large and bright (when labeled with a fluorescent dye such as SYBR Green I) that individual molecules were readily visualized with a fluorescence microscope. This was exploited to detect individual cleavage events subsequent to surface invasive cleavage. Two drawbacks of using RCA in the detection of individual cleavage events were the variability in the amplicon size, which results in a large variation in fluorescence signal intensity from the dye-labeled DNA molecules, and a high level of background fluorescence. Gold nanoparticles offer an excellent alternative to rolling circle amplification. Such particles are highly monodisperse with standard deviations in their diameters less than 10 %. This excellent monodispersity results in the production of uniform backscattering intensity from each particle when visualized with a scanning electron microscope. The two images in Figure 2 provide a side-by-side comparison between individual fluorescently tagged RCA molecules and individual gold nanoparticles. The S/N for individual fluorescently labeled RCA molecules was 33.5 ± 5.5 whereas the S/N for gold nanoparticles was 127.0 ± 1.1, a 4-fold improvement (see EXPERIMENTAL section “Calculations of Signal-to-Noise Ratio”). DNA, proteins and small molecules generate little background signal in scanning electron microscopy because these molecules are transparent to the electron beam. Gold particles, however, provide excellent signal in SEM images because the heavy gold atoms are capable of efficient electron scattering. The low background plays a large role in producing the high S/N in the SEM image. The standard deviations for the signal-to-noise ratios also indicate that the signal produced by backscatter from the nanoparticles is much more uniform than the signal produced by the individual RCA molecules. An added advantage of using gold nanoparticles as labels (compared to using fluorescent molecules) is that there is no phenomenon comparable to photobleaching in the SEM of gold while it can be a significant complicating factor in single molecule fluorescence imaging. Finally, gold nanoparticles imaged by SEM can be counted with high accuracy and confidence using freely available computer software packages whereas fluorescently tagged RCA amplicons cannot. The disadvantages of the SEM system as

compared to fluorescence microscopy are the lower availability of SEM instruments and the larger costs associated with their purchase, operation and maintenance.

Determining Detection Efficiency

The approach described above consists of successive steps of ligation of a biotin-tagged oligonucleotide to a free 5′-phosphate, binding of the biotinylated oligonucleotide to streptavidin-modified gold nanoparticles, and SEM imaging. In order to understand the overall efficiency of the process, the first two steps were analyzed separately. Surfaces were prepared using mixtures of oligonucleotides that were terminated at their 5′ ends either with dabcyl or with biotin. These biotin-terminated probes were identical to the molecules produced by ligation of biotinylated oligonucleotides to the surface-bound products of the invasive cleavage reaction. The dabcyl terminated probes were identical to the uncleaved probes used as starting material. The ratio of biotin-terminated probe relative to dabcyl terminated probe thus provides a simulated level of cleavage. All surfaces were prepared using the same total probe concentration. The number of hybridizable probes on the surfaces was determined using fluorescence wash-off experiments (Experimental section) [25] and was found to be (0.80±0.05) × 10^{12} molecules/cm^2. Five surfaces were analyzed with ratios of biotin/dabcyl of 1:1, 1:10, 1:100, 1:1000 and 1:10000 (Figure 3).

Randomly chosen regions from each of the images displayed in Figure 3 were selected for analysis. Bright spots, corresponding to gold nanoparticles, were counted automatically using NIH Scion Image processing software. A log-log plot of the particle density versus biotin probe density is displayed in Figure 4A. The density of bound nanoparticles scales linearly with biotin probe density up to ~1000 biotin probes/μm^2, the point at which particle crowding prevents complete labeling (see below). The efficiency of the binding between the streptavidin-modified gold nanoparticles and biotin is defined as the percentage of biotin groups that produced a detectable gold nanoparticle. The unadjusted range of apparent binding efficiencies fell between 5.20% and 69.9% (Figure 4B) and increased with decreasing density of biotin.

A similar approach was carried out to determine the ligation efficiency. Surfaces were prepared using mixtures of oligonucleotides terminated either in dabcyl or in phosphate. Five different mixtures were employed with ratios of phosphate/dabcyl of 1:1, 1:10, 1:100, 1:1000 and 1:10000. Degenerate template was employed in the ligation reaction to couple biotinylated oligonucleotides to surface immobilized oligonucleotides with free 5′ phosphate groups[12]. Following the ligation reaction, the surfaces were treated with streptavidin-coated gold nanoparticles. The number of particles per unit area was then calculated and divided by the number of surface bound phosphate groups. These values were then adjusted for the nanoparticle binding efficiency (see above) to arrive at the following percentages for ligation efficiency: 15.2; 20.8; 51.2; 56.8; and, 57.5 respectively. Efficiency was lowest for high phosphate density and highest for low phosphate density.

The efficiency of the complete nanoparticle labeling procedure (ligation followed by gold nanoparticle binding) is greater than that obtained from the complete RCA labeling procedure at all test surface phosphate densities (Table 1). The small size of the gold nanoparticles is an advantage over the RCA amplicons because there is less steric hindrance (see below). The data in Table 1 support this conclusion because the advantage in labeling efficiency is highest at high phosphate density where crowding of labels would be expected to have its largest influence. As the density of phosphate decreases, there is less advantage to having small size labels. A second explanation for the apparent improved labeling efficiency may be that the particles are more easily identified because of their strong, uniform electron backscattering. Short RCA amplicons may be undetectable because of the relatively high fluorescent backgrounds. Thus, many phosphates may be labeled but not detected by the RCA labeling scheme.

Particle Size Affects Nanoparticle Binding Efficiency

The efficiency of binding biotinylated probes with gold nanoparticles clearly declines as the density of biotin on the substrate increases [Figure 4B]. One hypothesis to account for this behavior is that at high surface densities of biotin, the spacing between adjacent biotin groups becomes smaller than the diameter of the gold nanoparticles and thus, only one of the two probes can be labeled. The probability *P* of finding two probes on a surface that are separated by a distance ≤ *r* where the average probe density is λ is given by Equation 1.[26,27]

$$P=Ae^{-\pi r^2\lambda} \quad (1)$$

Equation 1 yields a good fit to the experimental results (Figure 4B). In fitting this equation the value employed for *r* was 15 nm, the diameter of the nanoparticles. The value employed for the surface density λ was calculated based on the measured surface density of hybridizable oligonucleotides and the ratios of dabcylated and biotinylated thiol-oligonucleotides employed for preparation of the surface. The single free parameter *A* was fit to a value of 0.7. This value for *A* was surprising as it was expected to have a value of 1.[26,27] One possible explanation for this is that the real surface densities of biotinylated probes on the surface were lower by about 30% from the calculated values. There are several ways in which such a discrepancy could arise. First, some probes that were immobilized may have been lost from the surface during the normal course of reactions (ligation, incubation, conjugation, washing and drying).[28] Second, the efficiency of biotin-coupling during oligonucleotide synthesis is only about 90%, and the HPLC purification methods employed here do not separate the biotinylated oligonucleotides from unreacted non-biotinylated oligonucleotides. This means that the actual number of biotinylated probes is likely lower by ~10% than the calculated value. Finally, thiol groups on the oligonucleotides are known to dimerize, which can adversely affect their coupling to the surface. A larger fraction of dimerized biotinylated oligonucleotides than dimerized dabcylated oligonucleotides would lead to lower than calculated surface densities of biotin sites. Any or all of these issues could lead to a lower surface density of biotinylated oligonucleotides than calculated, which in turn would result in the lower apparent value for the preexponential factor *A*. In any event, it is clear from the results shown in Figure 4 that the efficiency of the gold nanoparticle binding to the surface biotin sites is close to unity when they are present at low surface concentration. This fact, taken together with the extremely low background levels and high contrast obtained from the SEM imaging of the nanoparticles, demonstrates the ability of the approach described here to detect and quantify individual surface sites.

Surface Invader System

A single polymorphism (W1282X) in the cystic fibrosis transmembrane conductance regulator (CFTR) gene 23 was chosen as a model system to develop and demonstrate this approach to SNP analysis. Wild-type and mutant-type allele-specific probes were immobilized on silicon chips. The upstream invader oligonucleotide and target DNA were included in the reaction buffer. Varying amounts of target DNA (see Table 2) were used to investigate the correspondence between the resulting signal and number of target molecules. The surface invader reaction was performed by incubating chips in either of two target solutions for 3 hours at 58.5 °C, along with Afu FEN enzyme (50 ng). Free 5′ phosphates were generated on the surface during the invasive cleavage reaction and then detected by ligation of biotinylated oligonucleotides to the free 5′ phosphate containing surface bound oligonucleotides using a degenerate template mixture. The surface was then treated with streptavidin-coated gold nanoparticles. The process is illustrated schematically in Figure 1. SEM images of the chips (following labeling) reveal that detected cleavage events scale linearly with the amount of target DNA (10^{-18}–10^{-15} moles) employed in the reactions (Figure 5). In addition, cleavage is specific for the type of target. An example of this is displayed in Figure 6 where cleavage

of mutant type probe occurred in the presence of mutant type target but not in the presence of wild type target.

This method of detection provides a straightforward approach to direct quantification of cleavage events and determination of cleavage efficiency and target cycling [7]. To evaluate the relationship between detectable particles and target DNA concentration and to determine the actual number of cleavage events per target, we performed surface invader reactions with varying target concentrations and plotted the number of detected particles per unit area against the number of target DNA molecules in the bulk reaction solution (see Figure 5 and Table 2). A more accurate determination of the number of cleavage events per target must take into account the efficiency of the ligation as well as the efficiency of the coupling between streptavidin and biotin with subsequent detection. Columns 3 and 4 of Table 2 display values for cleavage efficiency that take into account both of these factors. It is apparent from the data that target cycling occurs to a limited extent generating at most 4 cleavage events per target. Target cycling occurs to a much higher degree in the solution based invasive cleavage assay[7]. Work is in progress seeking to understand this difference.

CONCLUSION

Streptavidin coated gold nanoparticles offer many advantages over RCA amplicons for the detection of cleaved probes in the surface invasive cleavage assay. These advantages include: improved S/N; uniform intensity; low background levels; shorter labeling reaction times; and the ability to use software for confident automated particle counting. These advantages will be especially useful for the quantitative analysis of very low levels of analytes using the surface invasive cleavage assay and other surface-based assay systems.

Acknowledgements

We thank Third Wave Technologies (TWT) for providing the FEN enzyme and the design of the invasive cleavage assay for the CF mutations W1282X. LMS has a financial interest in TWT. This work was supported by NIH grants R01HG02298 and R01HG003275.

References

1. Wang W, Barratt BJ, Clayton DG, Todd JA. Nat Reviews Genetics 2005;6:109–118.
2. Kruglyak L. Nat Genet 1997;17:21–24. [PubMed: 9288093]
3. Stoneking M. Nature 2001;409:821–822. [PubMed: 11236996]
4. Thorisson GA, Stein LD. Nucleic Acids Res 2003;31:124–127. [PubMed: 12519964]
5. Chakravarti A. Nature 2001;409:822–823. [PubMed: 11236997]
6. Risch N, Merikangas K. Science 1996;273:1516–1517. [PubMed: 8801636]
7. Lyamichev V, Mast AL, Hall JG, Prudent JR, Kaiser MW, Takova T, Kwiatkowski RW, Sander TJ, de Arruda M, Arco DA, Neri BP, Brow MAD. Nat Biotechnol 1999;17:292–296. [PubMed: 10096299]
8. Eis PS, Olson MC, Takova T, Curtis ML, Olson SM, Vener TI, Ip HS, Vedvik KL, Bartholomay CT, Allawi HT, Ma W, Hall JG, Morin MD, Rushmore TH, Lyamichev V, Kwiatkowski RW. Nat Biotechnol 2001;19:673–676. [PubMed: 11433281]
9. Lyamichev V, Brow MAD, Varvel VE, Dahlberg JE. Proc Natl Acad Sci U S A 1999;96:6143–6148. [PubMed: 10339555]
10. Lyamichev V, Kaiser MW, Lyamicheva NE, Vologodskii AV, Hall JG, Ma W, Allawi HT, Neri BP. Biochemistry 2000;39:9523–9532. [PubMed: 10924149]
11. Hall JG, Eis PS, Law SM, Reynaldo LP, Prudent JR, Marshall DJ, Allawi HT, Mast AL, Dahlberg JE, Kwiatkowski RW, de Arruda M, Neri BP, Lyamichev VI. Proc Natl Acad Sci USA 2000;97:8272–8277. [PubMed: 10890904]
12. Chen Y, Shortreed MR, Olivier M, Smith LM. Anal Chem 2005;77:2400–2405. [PubMed: 15828773]

13. Nallur G, Luo C, Fang L, Cooley S, Dave V, Lambert J, Kukanskis K, Kinsmore S, Lasken R, Schweitzer B. Nucleic Acids Res 2001;29:23, e118.
14. Nie B, Shortreed MR, Smith LM. Anal Chem 2005;77:6594–6600. [PubMed: 16223245]
15. Levit-Binnum N, Lindner AB, Zik O, Eshhar Z, Moses E. Anal Chem 2003;75:1436–1441. [PubMed: 12659207]
16. Grubisha DS, Lipert RJ, Park HY, Driskell J, Porter MD. Anal Chem 2003;75:5936–5943. [PubMed: 14588035]
17. Nam JM, Thaxton CS, Mirkin CA. Science 2003;301:1884–1886. [PubMed: 14512622]
18. Taton TA, Mirkin CA, Letsinger RL. Science 2000;289:1757–1760. [PubMed: 10976070]
19. Brookes AJ. Gene 1999;234:177–186. [PubMed: 10395891]
20. Glen Research Corporation, User Guide to DNA Modification and Labeling. 1996.
21. Lu M, Hall JG, Shortreed MR, Wang L, Berggren WT, Stevens PW, Kelso DM, Lyamichev V, Neri B, Skinner JL, Smith LM. J Am Chem Soc 2002;124:7924–7931. [PubMed: 12095336]
22. Cai W, Zhang L, Strother T, Smith LM, Hamers RJ. J Phys Chem B 2002;106:2656–2664.
23. Knickerbocker T, Strother T, Schwartz MP, Russell JN Jr, Butler J, Smith LM, Hamers RJ. Langmuir 2003;19:1938–1942.
24. Chen Y, Shortreed MR, Peelen D, Lu M, Smith LM. J Am Chem Soc 2004;126:3016–3017. [PubMed: 15012108]
25. Peelen D, Smith LM. Langmuir 2005;21:266–271. [PubMed: 15620313]
26. Boots, BN.; Arthur, G. Point Pattern Analysis. Sage University; 1988.
27. Diggle PJ. Journal of the Royal Statistical Society A 1990;153:349–362.
28. Yang W, Auciello O, Butler JE, Cai W, Carlisle JA, Gerbi JE, Gruen DM, Knickerbocker T, Lasseter TL, Russell JN Jr, Smith LM, Hamers R. J Nat Mater 2002;1:253–257.

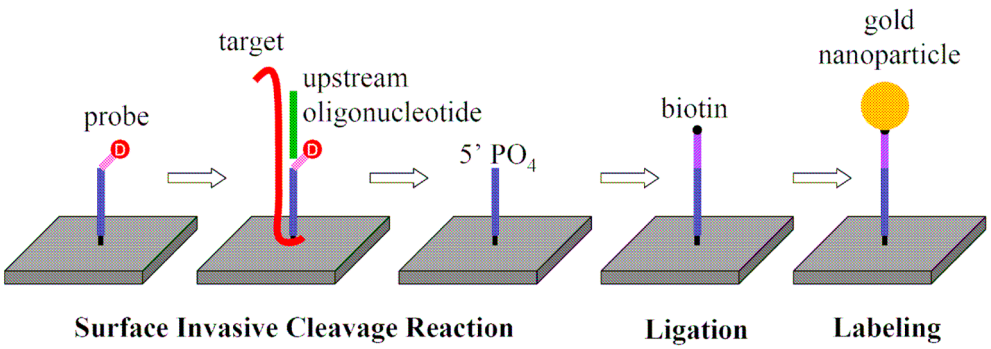

Figure 1.

Schematic illustration of surface invasive cleavage and nanoparticle labeling reactions. In invasive cleavage reactions, a three dimensional structure is formed by hybridization of two partially overlapping DNA oligonucleotides (referred to as probe and upstream oligonucleotides) to a target DNA strand. A flap endonuclease (FEN) specifically recognizes this structure and cleaves a flap from the probe oligonucleotide, which reveals a 5′ phosphate group that is used in a subsequent nanoparticle labeling reaction. Non-cleaved probes remain terminated with a 5′ dabcyl that was added during the oligonucleotide synthesis. The cleavage rate is greater if the nucleotide at the cleavage site of the flap is complementary to the opposing nucleotide on the target strand, conferring single nucleotide specificity to the cleavage reaction. Short biotinylated oligonucleotides are ligated to 5′ phosphate terminated oligonucleotides using a universal degenerate template whereas 5′ dabcyl terminated oligonucleotides are blocked from ligation. Finally, streptavidin-coated 15 nm gold nanoparticles are coupled to the surface immobilized biotin moieties.

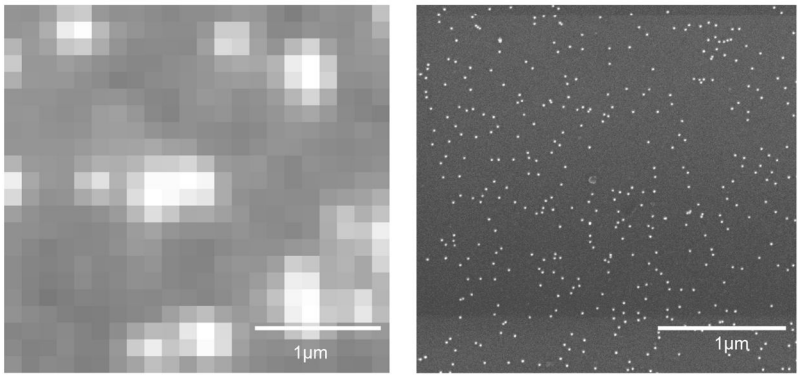

Figure 2.
Images of fluorescently tagged RCA amplicons obtained using an optical microscope and gold nanoparticles obtained using a scanning electron microscope. A) Products of the invasive cleavage reaction were labeled using degenerate ligation, rolling circle amplification and fluorescent stain according to the method described in Ref. 14. B) Products of the invasive cleavage reaction were labeled using degenerate ligation and conjugation to streptavidin coated gold nanoparticles.

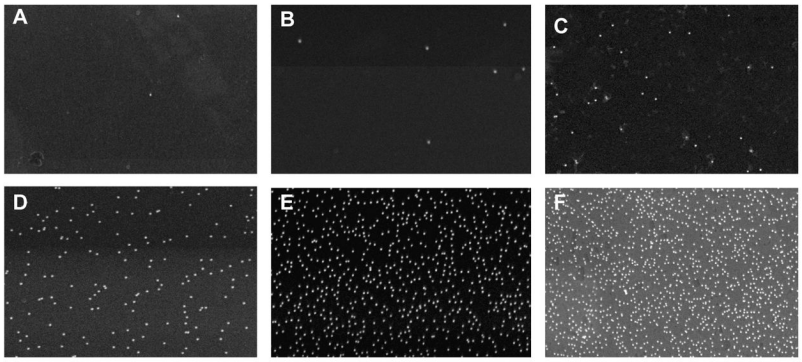

Figure 3.
SEM images of chips treated with streptavidin coated gold nanoparticles with a ratio of biotin to dabcyl of A) 0:1, B) 1:10000, C) 1:1000, D) 1:100, E) 1:10, and F) 1:1.

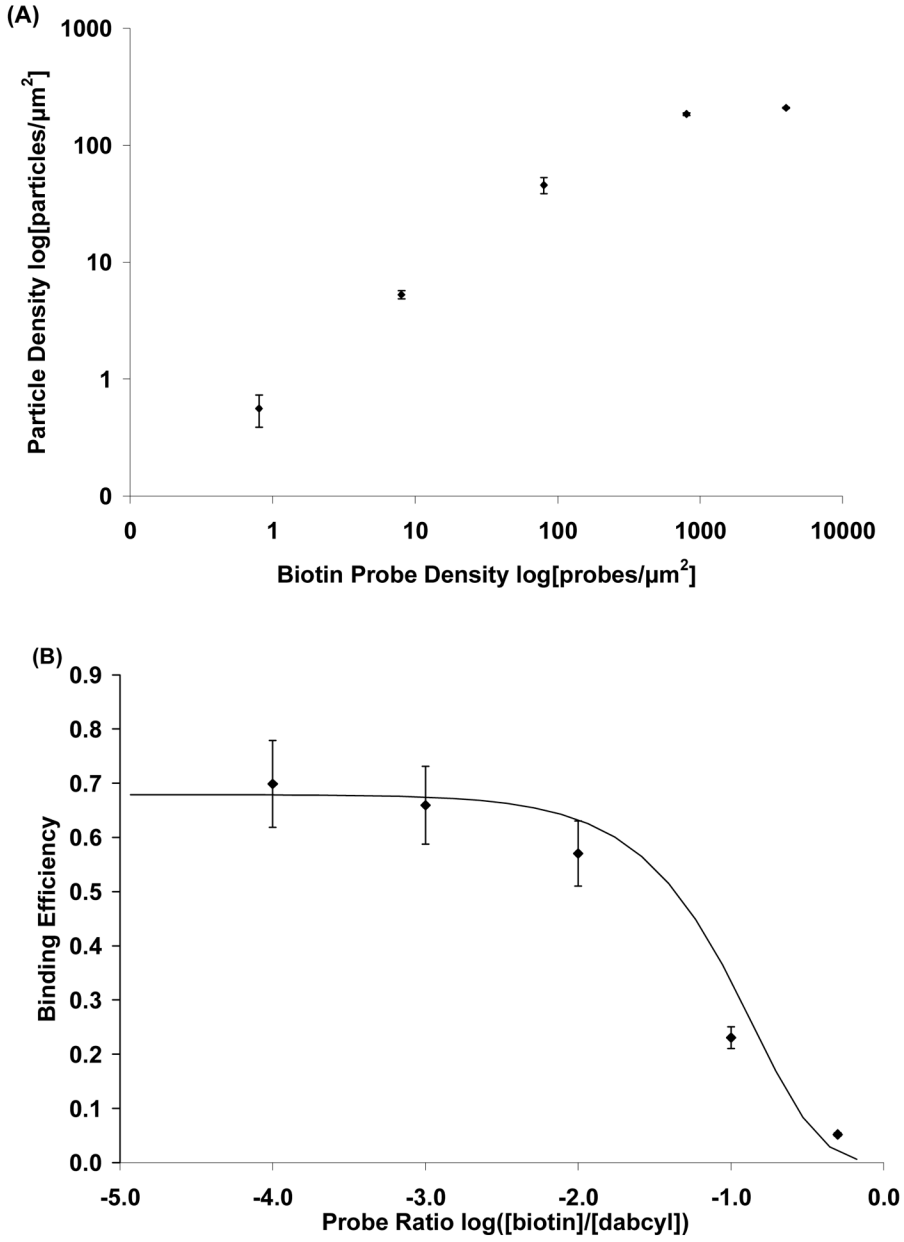

Figure 4.

A) The number of detected gold nanoparticles is a function of the ratio of biotin and dabcyl on surface. B) The calculated efficiency of detection depends on the ratio between the biotin and the dabcyl labeled oligonucleotide probes. Detection efficiency falls off as the ratio between biotin and dabcyl increases. The curve drawn in the Figure is a fit of Equation 1 to the experimental data.

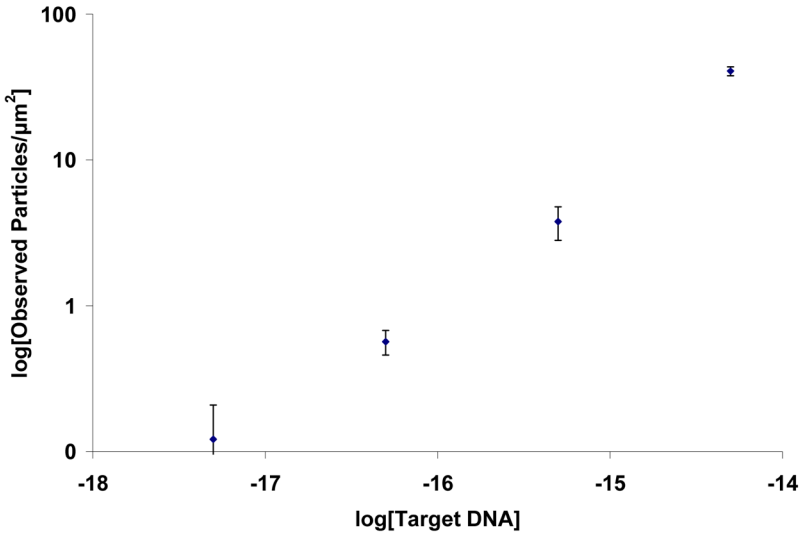

Figure 5.

The number of detected nanoparticles per μm^2 in a probe spot increases with the solution concentration of DNA target molecules present during the invasive cleavage reaction. The number of target molecules/μm^2 was calculated by dividing the number of target molecules in the reaction solution by the surface area of the chip.

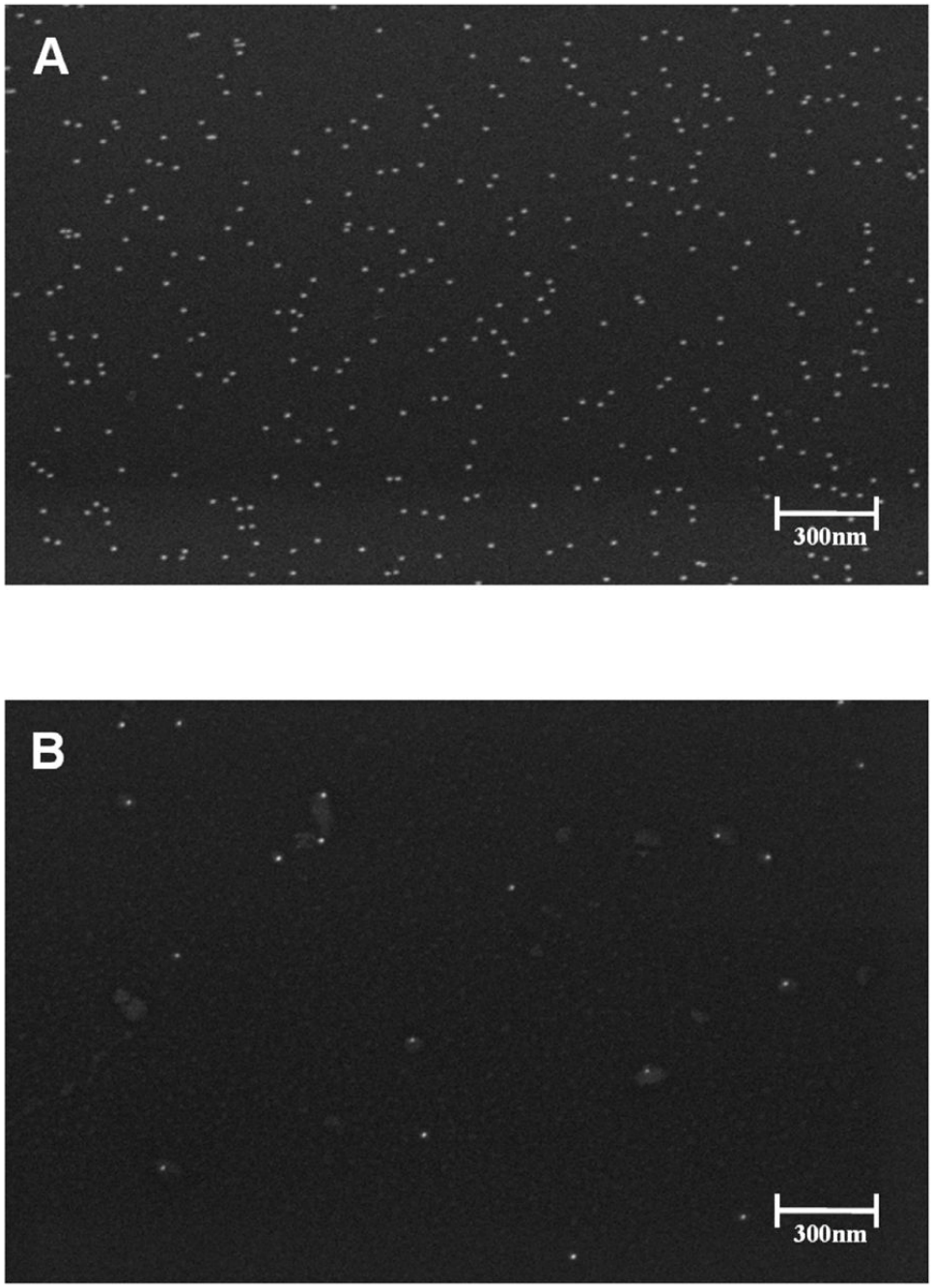

Figure 6.
Characteristic SEM images obtained from probe spots following surface invasive cleavage and nanoparticle labeling. A) Positive control reaction using mutant-type DNA target (5 fmol) and probe complementary to mutant-type, and B) negative control reaction using mutant-type DNA target and probe complementary to wild-type.

Table 1

The overall efficiency of both the nanoparticle and RCA labeling methods increased with decreasing phosphate surface coverage. The nanoparticle labeling is superior to RCA labeling at all tested phosphate densities. Data for column three was from Ref. 14.

Phosphate: Dabcyl Probe Ratio	Gold Nanoparticle Labeling Efficiency (%of labeled phosphate groups)	RCA Labeling Efficiency (% of labeled phosphate groups)[14]	Efficiency Improvement (Gold Efficiency/RCA Efficiency)
1:1	0.79 ± 0.04	-	-
1:10	4.8 ± 0.4	-	-
1:100	29.2 ± 3.5	1.9 ± 0.2	15.4 ± 2.4
1:1000	37.4 ± 4.5	4.7 ± 0.4	8.0 ± 1.1
1:10000	40.2 ± 6.4	8.8 ± 1.0	4.6 ± 0.9

Table 2

Average number of cleavage events per target molecule (column 2), adjusted for ligation efficiency (column 3), and adjusted for biotin/streptavidin conjugation efficiency (column 4). Details of the reaction can be found in the Experimental section under Surface Invasive Cleavage Reaction.

Amount of Target (amol)	Detected Cleavage Events per Target Molecule	Cleavage Events per Target Molecule Adjusted for Ligation Efficiency	Cleavage Events per Target Molecule Adjusted for Ligation and Conjugation Efficiency
5000	0.47 ± 0.04	1.3 ± 0.1	2.4 ± 0.2
500	0.44 ± 0.05	1.2 ± 0.2	2.2 ± 0.4
50	0.66 ± 0.07	1.0 ± 0.1	1.8 ± 0.2
5	1.4 ± 0.2	2.0 ± 0.3	3.9 ± 0.6
0	-	-	-